The Effects of Different Sudden Stratospheric Warming Type on the Ocean

Amee O'Callaghan,[1,2] Manoj Joshi,[1,2,3] David Stevens[1,4] and Daniel Mitchell[5].

Corresponding author: A. O'Callaghan, Climatic Research Unit, School of Environmental Sciences, University of East Anglia, Norwich Research Park, Norwich, Norfolk, United Kingdom. NR4 7TJ. (a.ocallaghan@uea.ac.uk)

[1]Centre for Ocean and Atmospheric Sciences, University of East Anglia. United Kingdom.

[2]School of Environmental Sciences, University of East Anglia. United Kingdom.

[3]Climatic Research Unit, University of East Anglia. United Kingdom.

[4]School of Mathematics, University of East Anglia. United Kingdom.

This article has been accepted for publication and undergone full peer review but has not been through the copyediting, typesetting, pagination and proofreading process, which may lead to differences between this version and the Version of Record. Please cite this article as doi: 10.1002/2014GL062179

There is a confirmed link between sudden stratospheric warmings (SSWs) and surface weather. Here we find significant differences in the strength of surface and ocean responses for splitting and displacement SSWs, classified using a new straightforward moment analysis technique. In an intermediate general circulation model splitting SSWs possess an enhanced ability to affect the surface climate demonstrating the need to treat the two types individually. Following SSWs the North Atlantic surface wind stress curl weakens, compared to its climatological winter state, for over 30 days: this is also evident in NCEP/NCAR reanalysis. The effect of anomalies associated with SSWs on the ocean is analysed in the IGCM4. The splitting SSW composite displays strong anomalies in the implied Ekman heat flux and net atmosphere-surface flux, modifying the mixed layer heat budget. Our results highlight that different SSW types need to be simulated in coupled stratospheric/tropospheric/ocean models.

[5]Department of Physics, University of Oxford. United Kingdom.

1. Introduction

During a major sudden stratospheric warming (SSW) the stratospheric polar vortex becomes greatly disturbed and the normal westerly flow regime is reversed [*Andrews et al.*, 1987]. There is a confirmed link between SSW events and the descent of negative Northern Annular Mode index (NAM) anomalies [*Baldwin and Dunkerton*, 2001] which can modify the surface climate at mid-high latitudes [*Mitchell et al.*, 2013, (hereafter M13)]. However, little work has been conducted into the potential effect on ocean circulation. *Reichler et al.* [2012] demonstrated the interaction of strong polar vortex events with the North Atlantic Ocean through surface wind stress anomalies and latent and sensible heat flux. This was conducted in a model with low stratospheric variability when compared to the National Centers for Environmental Prediction National - Center for Atmospheric Research (NCEP/NCAR) reanalysis. There is also a link, demonstrated by *Marshall et al.* [2001] and *Zhai et al.* [2014], between the phase of the surface NAM and ocean circulation communicated via downwelling rates and Ekman dynamics. A key question is: how do anomalies associated with SSWs make their way into the ocean system and is the response dependent on SSW type? The purpose of this study is to investigate the surface impacts associated with the two main types of SSWs; splitting and displacement events. Particular focus will be on the surface wind stress and the net atmosphere-surface flux that lead to changes in the mixed layer heat budget. This work follows that of *Reichler et al.* [2012] but from a new perspective of the influence of different SSW types on the ocean. An atmosphere-only general circulation model is utilised to isolate the direct influence of SSW events.

2. The IGCM4 and Methodology

The Intermediate General Circulation Model (IGCM) is a primitive equation atmospheric model which uses spherical geometry. It is based on the baroclinic model of Hoskins and Simmons with the developmental history of the first version summarised by *Blackburn* [1985].

The IGCM4 is implemented with a horizontal resolution of T42, approximately 2.8°, and run for a 200 year period. There are 35 sigma levels with a model lid at 0.1 hPa. There are 3 sigma levels above 1 hPa, 13 in the stratosphere and 19 in the troposphere. Ozone and sea surface temperatures are prescribed monthly using climatologies of monthly means. A gravity wave drag scheme is utilised based on *Lindzen* [1981] which conserves momentum. December to February climatologies are produced and compare favourably to a climatology derived from ERA-40 data between 1959 and 2002 [*Uppala et al.*, 2005]. The daily variability of zonal winds in the IGCM4, poleward of 30°N, is comparable to reanalysis. For further details on the IGCM4 see *Joshi et al.* [2014].

2.1. SSW Identification and Classification Algorithm

The SSW identification algorithm is based upon the technique of *Charlton and Polvani* [2007], hereafter CP07. This isolates SSW 'central dates' when the zonal mean zonal wind at 10hPa and 60°N reverses and becomes easterly. Final warmings and duplicates of SSW central dates are also removed following CP07. The winter period is reduced to December-March to avoid Canadian Warmings. There is one additional criterion included to ensure there is a warming poleward of 50°N to adhere more closely to the WMO definition. Spatial averages of the temperature field are calculated for the regions 50-70°N and 70-

90°N at 10hPa. If the polar region is colder than the surrounding area then the WMO criterion is violated and this central date is removed. This method isolates 113 events which are further subdivided into splits and displacements using 2D moment analysis applied to potential vorticity on the 850 $K\theta$-level.

Mitchell et al. [2011] successfully used moment analysis to describe SSWs; the methodology is in turn based upon works by *Waugh* [1997], *Waugh and Randel* [1999] and *Matthewman et al.* [2009]. A moment is the quantitative measure of the shape of a set of two-dimensional data points. *Matthewman et al.* [2009] further developed the equations to include kurtosis. A kurtosis of 1 describes a Gaussian distribution, a lower or negative kurtosis indicates a large spread around the centre of the polar vortex which is indicative of a splitting event. The condition set to define a SSW split event is a drop in kurtosis below -0.1 in the 20 days surrounding the zonal mean zonal wind reversal at 10hPa and 60°N (following *Matthewman et al.* [2009]); otherwise the event is a displacement.

2.2. SSWs in the IGCM4

SSWs are identified and classified, as outlined in section 2.1, and benchmarks formulated by CP07 are used to assess SSWs in the IGCM4. Overall the 113 events yield a frequency of 0.57 (0.05) events per year, with standard error in parentheses. This falls within the benchmark of 0.6 (0.1) events per year. The meridional heat flux (averaged over the 20 days leading up to the event dates and between 45°N and 75°N) is a proxy for the wave activity entering from the troposphere and is also within standard error of the CP07 value at 7.1 (0.4) K m s^{-1} compared to the benchmark of 8.5 (1.0) K m s^{-1}. There are 48 splitting SSWs and 65 displacements. The ratio of splits to displacements is 0.74 and

is close to the value found in CP07 of 0.86. The overall strength of events at 10 hPa, measured by the deceleration of zonal wind and warming of the polar cap, is slightly weak. The average wind deceleration at 60°N and 10 hPa is calculated as the difference in zonal mean zonal wind from 15 to 5 days prior to the central date minus that from 0 to 5 days after the central date. For both SSW types the average deceleration is 20.2 (0.7) m s^{-1} this is outside the benchmark of 26.2 (1.8). Coupling with the troposphere is of the correct magnitude with an average 100 hPa polar cap temperature anomaly, between 90°N and 50°N and 5 days around the central date, of 1.9 (0.1) K which is within the benchmark of 2.0 (0.3) K. This displays that the disturbance in the stratospheric polar vortex is descending into the troposphere and has an adequate strength.

2.3. Variable Formulation

Climatologies are calculated by averaging over individual days and anomalies are taken as departures from the climatology to remove seasonality. The bulk aerodynamic formula presented in *Forster et al.* [2000] is applied over the ocean to compute the surface wind stress. From this the vertical component of curl is taken to formulate the surface wind stress curl.

To view the surface impacts following SSWs, anomaly fields are averaged from event onset (lag 0) to 30 days after (lag +30) and labelled the *mature stage* following M13. A further stage is assessed from 30 to 60 days (lag +60) following the events and is termed the *decay stage*.

The NAM anomaly is formulated directly from daily zonal mean geopotential height anomalies poleward of 20°N, following the work of *Baldwin and Thompson* [2009] and is

optimised to assess daily stratosphere-troposphere coupling. The NAM anomaly at each model level is then rescaled to have unit variance [*Mitchell et al.*, 2013] allowing for direct comparison throughout the entire atmospheric column.

Composites of anomaly fields are produced for the identified split and displacement events to determine the average behaviour following a SSW and the difference is calculated by subtracting the displacement from the splitting composite. A paired students t-test (or a Welch's test for unequal sample variances) is used to assess the probability that the anomalies would occur given that the null hypothesis was true. For anomaly fields the null hypothesis states that there is no difference between the anomaly data surrounding a SSW event (for the time frame of interest) and the anomaly data averaged for each winter season. This test assesses the probability that the anomalies surrounding the SSW events are typical of winter behaviour and could have occurred randomly. If this chance is less than 5% the data is stippled and not insignificant. For the difference fields (split composite minus displacement) a paired t-test is used with a null hypothesis that there is no difference between the splitting and displacement composites, again p-values of less than 0.05 are stippled.

3. Results

3.1. NAM Anomaly

The descent of NAM anomalies associated with splitting and displacement SSWs is presented in Figure 1 and should be compared to Figure 4 of M13 who investigated surface impacts following SSWs in ERA-40 reanalysis. Our results show similarities with M13. In the stratosphere there is a positive anomaly leading up to event onset, lag 0,

which is stronger for displacements. The negative anomaly appears before lag 0 in both cases and peaks just after an event occurrence in the middle stratosphere. The difference between splitting and displacement composites is displayed in Figure 1(c). The negative anomaly leading up to lag 0, throughout the entire atmospheric column, is significantly stronger for the splitting composite. The maximum strength in the middle stratosphere at lag 0 is around -3 for displacements and -2.5 for splits which is significantly different. The displacement composite may have more impact in the middle stratosphere, at lag 0, but possesses less ability to descend to the surface. For the splitting composite there is a persistent negative surface anomaly appearing just prior to event onset and lasts for over 30 days. It has a peak strength of around -1. The surface impact in the displacement composite is significantly weaker and more intermittent. The displacement peak impact occurs in the decay period (lag +30 to +60). Splitting events have a heightened ability to affect the surface climate in the IGCM4, this is insensitive to the number of ensemble members and shows similar, albeit noisier, behaviour when composite plots are created using SSW events having central dates in one particular winter month. Negative NAM anomalies have similar life spans in the stratosphere for both types of SSW, although appear to last slightly longer for splits. In both cases there is a return to normal conditions 60 days after an event.

The NAM anomaly behaviour in the IGCM4 is similar to the findings of M13. However, there is a difference worthy of noting. For the splitting composite the anomaly descent from the tropopause to the surface is far quicker in the model that in ERA-40, where NAM anomalies take 15 days to reach the surface. The peak negative anomalies occur in

the decay phase in the reanalysis and it is evident that the timescales for descent in the IGCM4 are faster than in ERA-40.

3.2. Wind Stress Curl

NAM anomalies are often associated with surface wind stress anomalies which are important in driving a dynamical response in the ocean. *Marshall et al.* [2001] and *Zhai et al.* [2014] showed that meridional shifts in the zero surface wind stress curl line associated with NAO anomalies (closely related to the surface NAM [*Solomon et al.*, 2007]) drive long-term anomalous circulations in the North Atlantic Ocean. Shorter-term NAM anomalies do also impact the ocean system as found in *Reichler et al.* [2012]. Here we examine the differences in ocean impact depending on if a splitting or displacement SSW event occurs.

We analyse the post-SSW surface state in the IGCM4 and also in NCEP/NCAR reanalysis (T62 with 28 vertical levels) [*Kalnay et al.*, 1996], the latter using event dates isolated in CP07. There are a total of 27 NCEP/NCAR SSW events located in CP07 with one occurring in November which is discarded. The surface wind stress curl anomaly fields are presented in Figures 2(a) and (b) for the IGCM4 and NCEP/NCAR reanalysis respectively. Once again the timescale for anomaly onset is faster in the model. The period with the strongest anomalies is presented (when averaging over lag 0 to +60 the anomaly pattern is still evident and significant but weaker). Figure 2 shows good agreement between model and reanalysis with both displaying negative NAM anomaly responses primarily over the North Atlantic Ocean. This acts to weaken the climatological pattern (by around 30% in the IGCM4) and pulls the zero wind stress curl line equatorward in both the model

and reanalysis. A cyclonic anomaly across the boundary between the sub-polar gyre and sub-tropical gyre appears in agreement with the work of *Marshall et al.* [2001]. The shift in the zero wind stress curl line should result in a more zonal North Atlantic Current.

3.3. Surface Energy Flux

The anomalous behaviour in the surface wind stress, highlighted in section 3.2, is communicated into the ocean on short (up to 60 day) timescales both dynamically and thermodynamically. In particular surface wind stress anomalies lead to Ekman transport variations that induce upper ocean heat transport convergences. This transport convergence is expressed as an implied Ekman heat flux following *Marshall et al.* [2001] and *Visbeck et al.* [2003]. The other atmospheric surface flux terms are; surface longwave radiation, surface shortwave radiation, surface latent and sensible heat terms. In this paper the combination of these four atmospheric surface fluxes are called the net atmosphere-surface flux.

The implied Ekman heat flux and the net atmosphere-surface flux are modified following a SSW and their sum is labelled the combined upper ocean energy flux.

The anomalous net atmosphere-surface flux for the mature period in the IGCM4 is shown in Figure 3. Behaviour in the decay period is similar and weaker. We now determine if the surface response is different between the two types of SSW in the IGCM4. Composite anomalies following 48 splitting events are presented in the left hand column of Figure 3 for; 3(a) the net atmosphere-surface flux (surface shortwave and longwave radiation and surface latent and sensible heat terms), 3(d) the implied Ekman heat flux, formulated following *Marshall et al.* [2001], and (g) their sum the combined upper ocean energy flux.

The anomalies in the North Atlantic Ocean have similar spatial patterns for the splitting and displacement composites. However, the magnitude is different with the displacement composite anomalies being, at most, half the strength when compared to the splitting events. This difference is significant between 45°N and 75°N for all three flux fields, as shown in Figures 3(c), (f) and (i). This suggests that splitting and displacement SSWs should be considered as distinct events. This is consistent with the conclusions of M13 who found that there was a need to identify vortex splitting and displacement events individually if an accurate understanding of influence on the surface climate was to be achieved.

For the splitting SSWs the surface fluxes in the North Atlantic Ocean following event onset are strong and would modify the mixed layer heat budget (see Equation 4 of *Screen et al.* [2010]). The net atmosphere-surface flux, Figure 3(a), displays anomalous fluxes into the ocean over the sub-polar gyre and out of the ocean over the sub-tropical gyre. This anomalous pattern is slightly different in the implied Ekman heat flux, Figure 3(c), which is weaker and shifted equatorward. The implied Ekman heat flux provides a non-negligible contribution. The combined upper ocean energy flux, Figure 3(e), has strong anomalous fluxes, over 50 W m^{-2}, into the ocean between 65°N and 40°N and anomalous fluxes out of the ocean, up to 40 W m^{-2}, from 40°N to 25°N. Note that once the net atmosphere-surface flux is considered in conjunction with the implied Ekman heat flux the transition between anomalous positive and negative flux is shifted equatorward. This is important because the Ekman response acts to 'pull' the positive flux into the ocean towards regions of shallower mixed layer depth enabling the anomaly to have a more

significant impact on the ocean heat budget. Overall the signal is one of cooling in the sub-tropical gyre and warming in the sub-polar gyre with exact magnitude of change being dependent on the local mixed layer depth. A more detailed quantification of this impact requires a coupled atmosphere-ocean general circulation model that takes into account both dynamic (implied Ekman heat flux) and thermodynamic (net atmosphere-surface flux) ocean heating, as well as spatial variations in mixed layer depth.

4. Discussion and Conclusions

We have investigated splitting and displacement sudden stratospheric warmings in the IGCM4; a model which represents the stratospheric circulation and SSW behaviour well. There is a heightened ability for anomalies associated with splitting events to descend into the troposphere and reach the surface. There are negative NAM anomalies in the troposphere for the splitting composite which last for over 30 days. This behaviour is consistent with the findings of *Mitchell et al.* [2013] but the timescales are different. Anomalies in the IGCM4 rapidly travel through the atmospheric column and reach the surface whereas this takes up to 15 days in reanalysis. This timescale difference is also observed in the surface fields.

In both the IGCM4 and NCEP/NCAR reanalysis datasets there is a weakening of the climatological winter surface wind stress patterns following SSW events. In the IGCM4 there are significant anomalies in the surface wind stress following SSWs, which are stronger for the splitting composite, providing a pathway for SSWs to interact with ocean dynamics. The surface wind stress anomalies generate anomalous implied Ekman heat fluxes which, once combined with the net atmosphere-surface fluxes, alter the mixed layer heat budget.

This work shows that the source of memory from ocean impacts following SSWs is mainly due to splitting events which could be useful in interpreting other model results that show an ocean response to stratospheric forcing (e.g. *Scaife et al.* [2013]). The displacement events do not have the same impact on the surface climate and ocean; this is consistent with the results of *Mitchell et al.* [2013]. When considering ocean impacts splitting and displacement SSWs should be considered as separate phenomena. *Reichler et al.* [2012] assessed the surface and ocean responses following strong polar vortex events (in a sense a comparable phenomenon to SSWs but with the opposite magnitude). This study finds a similar spatial pattern in the anomalous surface fluxes but also includes the radiative and implied Ekman transport induced terms to provide a more complete understanding of the surface flux behaviour.

Our results highlight the need for different SSW types to be simulated in coupled stratospheric/tropospheric/ocean models. While this paper has focused on the impacts from the atmosphere into the ocean, a fully coupled model would provide more insight into how these anomalies interact and propagate in a dynamical ocean and also include potential feedback mechanisms.

Acknowledgments. We are grateful for fruitful discussions with Xiaoming Zhai, David Ferreira and Andrew Charlton-Perez. The ERA-40 data were obtained from the ECMWF data server at http://data−portal.ecmwf.int/data/d/era40_moda/levtype=pl/. NCEP Reanalysis data provided by the NOAA/OAR/ESRL PSD, Boulder, Colorado, USA, from their web site at http://www.esrl.noaa.gov/psd/. We are very grateful for the provision of these freely available online resources. The research presented in this paper

was carried out on the High Performance Computing Cluster supported by the Research and Specialist Computing Support service at the University of East Anglia. AO and DMM are both independently supported by the UK Natural Environmental Research Council.

References

Andrews, D., J. Holton, and C. Leovy (1987), *Middle Atmosphere Dynamics*, Academic Press.

Baldwin, M., and T. Dunkerton (2001), Stratospheric harbingers of anomalous weather regimes, *Science*, *294*, 581–584.

Baldwin, M., and D. Thompson (2009), A critical comparison of stratosphere–troposphere coupling indices, *Q.J.R. Meteorol. Soc.*, *135*, 1661–1672.

Blackburn, M. (1985), Program description for the multi-level global spectral model.

Charlton, A., and L. Polvani (2007), A new look at stratospheric sudden warmings. part I: Climatology and modeling benchmarks, *J. Climate*, *20*, 449–469.

Charlton, A., L. Polvani, J. Perlwitz, F. Sassi, E. Manzini, K. Shibata, S. Pawson, J. Nielsen, and D. Rind (2007), A new look at stratospheric sudden warmings. part II: Evaluation of numerical model simulations, *J. Climate*, *20*, 470–488.

Forster, P., M. Blackburn, R. Glover, and K. Shine (2000), An examination of climate sensitivity for idealised climate change experiments in an intermediate general circulation model, *Clim. Dyn.*, *16*, 833–849.

Joshi, M., M. Stringer, K. van der Wiel, A. O'Callaghan, and S. Fueglistaler (2014), IGCM4: A fast, parallel and flexible intermediate climate model, *Geosci. Model Dev. Discuss.*, *7*, 5517–5545.

Kalnay, E., M. Kanamitsu, R. Kistler, W. Collins, D. Deaven, L. Gandin, M. Iredell, S. Saha, G. White, J. Woollen, Y. Zhu, A. Leetmaa, R. Reynold, M. Chelliah, W. Ebisuzaki, W. Higgins, J. Janowiak, K. Mo, C. Ropelewski, J. Wang, R. Jenne, and D. Joseph (1996), The NCEP/NCAR 40-year reanalysis project, *Bull. Amer. Meteor. Soc.*, *77*, 437–471.

Lindzen, R. (1981), Turbulence and stress owing to gravity wave and tidal breakdown, *J. Geophys. Res.*, *86*, 9707–9714.

Marshall, J., H. Johnson, and J. Goodman (2001), A study of the interaction of the North Atlantic Oscillation with ocean circulation, *J. Climate*, *14*, 1399–1421.

Matthewman, N., J. Esler, A. Charlton-Perez, and L. Polvani (2009), A new look at stratospheric sudden warmings. part III: Polar vortex evolution and vertical structure, *J. Climate*, *22*, 1566–1585.

Mitchell, D., A. Charlton-Perez, and L. Gray (2011), Characterizing the variability and extremes of the stratospheric polar vortices using 2D moment analysis, *J. Atmos. Sci.*, *68*, 1194–1213.

Mitchell, D., L. Gray, J. Anstey, M. Baldwin, and A. Charlton-Perez (2013), The influence of stratospheric vortex displacements and splits on surface climate, *J. Climate*, *26*, 2668–2682.

Reichler, T., J. Kim, E. Manzini, and J. Kroger (2012), A stratospheric connection to Atlantic climate variability, *Nature Geosci.*, *5*, 783–787.

Scaife, A., S. Ineson, J. Knight, L. Gray, K. Kodera, and M. Smith (2013), A mechanism for lagged North Atlantic climate response to solar variability, *Geophys. Res. Lett.*, *40*,

434–438.

Screen, J., N. Gillett, A. Karpechko, and D. Stevens (2010), Mixed layer temperature response to the southern annular mode: Mechanisms and model representation, *J. Climate*, *23*, 664–678.

Solomon, S., D. Qin, Z. Chen, M. Marquis, K. Averyt, M. Tignor, and H. Miller (Eds.) (2007), *Contribution of Working Group I to the Fourth Assessment Report of the Intergovernmental Panel on Climate Change, 2007*, Cambridge University Press.

Uppala, S., P. Kallberg, A. Simmons, U. Andrae, V. Bechtold, M. Fiorino, J. Gibson, J. Haseler, A. Hernandez, G. Kelly, X. Li, K. Onogi, S. Saarinen, N. Sokka, R. Allan, E. Andersson, K. Arpe, M. Balmaseda, M. Beljaars, L. Van De Berg, J. Bidlot, N. Bormann, S. Caires, F. Chevallier, A. Dethof, M. Dragosavac, M. Fisher, M. Fuentes, S. Hagemann, E. Holm, B. Hoskins, L. Isaksen, P. Janssen, R. Jenne, A. Mcnally, J. Mahfouf, J. Morcrette, N. Rayner, R. Saunders, P. Simon, A. Sterl, K. Trenberth, A. Untch, D. Vasiljevic, P. Viterbo1, and J. Woollen (2005), The ERA-40 re-analysis, *Q.J.R. Meteorol. Soc.*, *131*, 2961–3012.

Visbeck, M., E. Chassignet, R. Curry, T. Delworth, R. Dickson, and G. Krahmann (2003), The ocean's response to North Atlantic Oscillation variability, in the North Atlantic Oscillation: Climatic significance and environmental impact, *Am. Geophys. Un. Mon.*, *134*, 113–145.

Waugh, D. (1997), Elliptical diagnostics of stratospheric polar vortices, *Q. J. R. Meteorol. Soc.*, *123*, 1725–1748.

Waugh, D., and W. Randel (1999), Climatology of Arctic and Antarctic polar vortices using elliptical diagnostics, *J. Atmos. Sci.*, *56*, 1594–1613.

Zhai, X., H. Johnson, and D. Marshall (2014), A simple model of the response of the Atlantic to the North Atlantic Oscillation, *J. Climate*, *27*, 4052–4069.

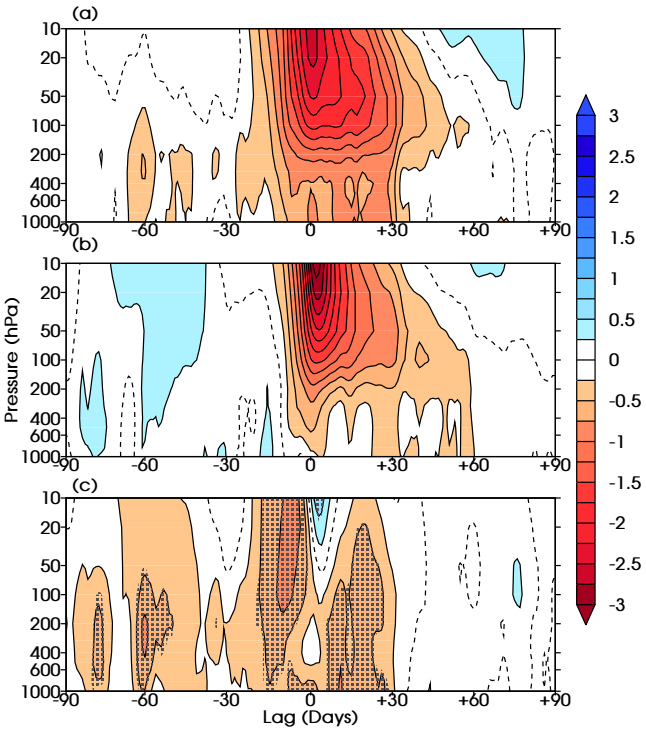

Figure 1. The NAM anomaly (unitless) in the IGCM4 for 90 days surrounding identified SSWs as a function of height against time for: (a) 48 splitting events composite and (b) 65 displacement events composite. (c) splitting composite minus displacement composite where stippling represents a p-value of less than 5%. The dashed line represents the zero contour. The NAM index anomaly is both unitless and dimensionless.

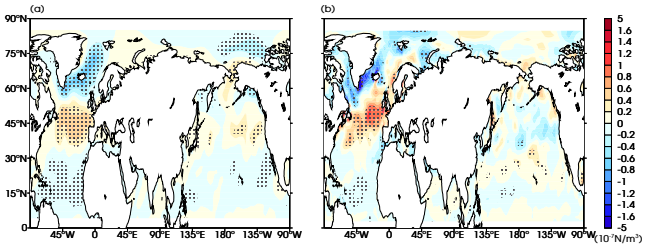

Figure 2. Surface wind stress curl anomaly composites (10^{-7} N m^{-3}) for: (a) 113 SSWs in IGCM4 mature period (lag 0 to lag +30) and (b) 26 CP07 SSWs in NCEP/NCAR reanalysis decay period (lag +30 to lag +60). Stippling represents a p-value of less than 5%.

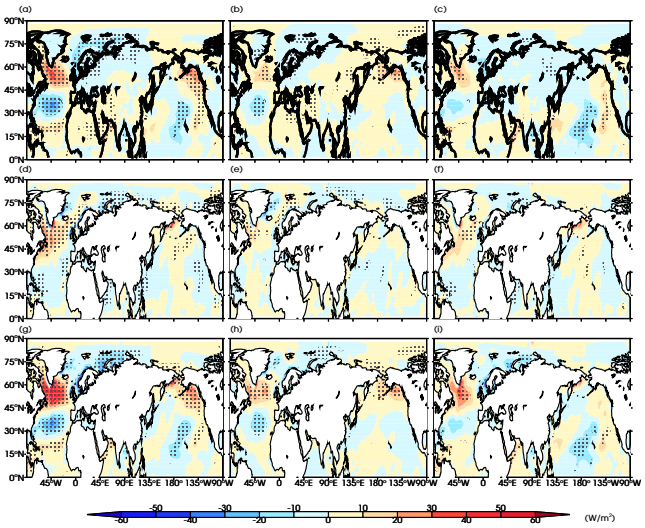

Figure 3. Mature period (lag 0 to lag +30) IGCM4 composites for splitting anomalies, displacement anomalies and their difference (splittings minus displacements) in columns one, two and three respectively for; (a)-(c) net atmosphere-surface flux, (d)-(f) implied Ekman heat flux and (g)-(i) the combined upper ocean energy flux. Positive fluxes are into the planet (downwards) units are in Wm^{-2}. There are 48 splitting events (left column) and 65 displacement events (middle column). Stippling represents a p-value of less than 5%.